

Surface and volume photoemission from metal nano-particles with electron mass discontinuity

I.E.Protsenko and A.V.Uskov

Quantum Electronic division, Lebedev Physical Institute Moscow, Russia 119991

October 29, 2020

Abstract

Quantum efficiencies of surface (SPE) and volume (VPE) photo-emissions from metal nanoparticles are calculated by quantum mechanical perturbation theory and compared with each other. Along with discontinuities in the potential barrier and dielectric function, the discontinuity in electron effective mass on the metal-environment interface is taken into account. General formulas for quantum efficiencies of SPE and VPE are derived. An example of spherical gold particles with rectangular potential barrier on the interface is considered, analytical formulas for quantum efficiencies of SPE and VPE on the red border of photoemission are derived. It is found that the efficiency of SPE decreases with the reduction of the electron effective mass slowly than the efficiency of VPE and SPE is more efficient than VPE for small particles, large discontinuity in effective mass and not too high photon energies. Nanoparticle size when SPE is more efficient than VPE is found to be tens of nm or less.

Keywords: surface photo-emission, hot electrons, metal nano-particles

I. INTRODUCTION

A photon of electromagnetic field in a metal can be absorbed at the collision of an electron with impurity, lattice defect or with the metal surface [10]. If the energy of electron after absorption of photon overcomes the potential barrier on the interface, the electron may be emitted from the metal. In metal nano-particles at certain conditions high-energy electrons, generated by photo-absorption, become "hot": they are thermalized and form an ensemble characterized by a model carrier density and a distribution with high temperature [11]. Hot electrons find various applications [3], and the increase of efficiency of hot electron emission is topical but difficult problem depended on many factors. In particular, hot electron emission from nanoparticle is strongly reduced because of electron effective mass difference in the semiconductor environment and in the metal [8]. A possibility to increase hot electron emission from metal nanoparticles is to use photoemission from the surface of particles, see [15] and references therein, which is confirmed by recent experiments [6].

Absorption of electromagnetic field at collisions of electrons with the metal-environment interface and emission of such electrons have been studied for a long time [14]. Two processes are possible at the interaction of an electron and a photon on the surface [2]. One process is a surface photo-emission (SPE), when an electron collides with a potential barrier, absorbs a photon and leave a metal. Another process is when an electron absorbs photon and came back to a metal, this is surface photo-absorption (SPA) process.

It is well-known that discontinuities in the potential barrier, electromagnetic field and electron effective mass on the interface strongly influence SPE and SPA [1, 2]. General approach for SPE in metal nanoparticles, taking into account discontinuities in electromagnetic field and electron effective mass is given in [13] following the description of SPE by quantum theory of periodic perturbations in continues spectrum [1, 2]. The approach and results of [13] have been used, in particular, for studies of electron photoemission from plasmonic nanoantennas [12], comparison between surface and volume photoelectric effects in the internal photoemission from plasmonic nanoparticles [15], broadening of plasmonic resonance due to electron collisions with nanoparticle boundary [16] and enhanced electron photoemission by collective resonances in the nanopartical lattices [17].

Comparison between the surface and the volume photoemission in metal nanoparticles have been made in [15] without taking into account discontinuity in electron effective mass on the metal-environment interface. The main purpose of this paper is to extend [15] and compare SPE and VPE taking into account the discontinuity of electron effective mass. Such comparison will help to find conditions for the most efficient emission of hot electrons from metal nanoparticles. Another purpose is to extend the study of SPE in [13] to SPA and provide ready-to-use formulas for efficiencies of SPE and SPA, also for non-rectangular potential barriers. SPA is important for broadening of surface plasmon resonances in nano-particles [7]; for correct estimations of heating of metal nano-structures necessary, for example, for various medical applications [9].

In the Section II we consider surface photoemission and, following [13], present general formula for probabilities of SPE and SPA with discontinuities in the electron mass and electromagnetic field on the surface, taking into account the structure of potential barrier on the interface. We apply general formulas for SPE for rectangular potential barrier taking into account discontinuity in electron effective mass.

In the Section III we, following the approach of [15], present general formulas for volume

photoemission with discontinuity of electron effective mass on the interface and apply them to a case of rectangular potential barrier on the surface of metal nanoparticle. We restrict ourselves by small spherical particles with uniform electric field inside.

In Sections II and III we provide analytical formulas for quantum efficiencies of SPE and VPE near the red border of photoemission and for estimations of the maximum size of nanoparticles, when SPE is comparable with VPE.

In Section IV we compare efficiencies of the volume and the surface photoemission on examples of gold nanoparticles in semiconductor environment with rectangular-step potential barrier on the interface. We discuss and explain the results of the comparison. We summarize results in Summary section.

II. SURFACE PHOTOEMISSION

Suppose an electron in metal moves toward the interface between a metal and a semiconductor. There is electromagnetic field of frequency ω inside and outside the metal. Following the approach of [1] we consider, first, one-dimensional (1D) problem. We describe the interface by one-dimension potential barrier $V(z)$ shown on Fig.1. The electron reaches the interface, collides with the barrier and absorbs, with some probability, a photon from the field. Only the component of external field normal to the interface interacts with the electron. The electron can pass the barrier, leave the metal, and contribute to a surface photo-emission, SPE, with a probability amplitude C_+ . Otherwise, the electron can be reflected from the barrier back to the metal with a probability amplitude C_- and contribute to the surface photo-absorption SPA.

A. Results for 1D case

The interaction of an electron with the electromagnetic field is a perturbation. Final state ψ_1 of an electron after absorption of a photon is $\psi_1 = C_+ \Psi_{1+} + C_- \Psi_{1-}$, where $\Psi_{1\pm}$ are unperturbed wave-functions of the electron moving in the potential $V(z)$ without electromagnetic field. We found probability amplitudes of SPE C_+ and SPA C_-

$$C_{\pm} = c_{\pm} \mathcal{E}_{in}^{(n)} = \left(c_{\pm}^{(0)} - \frac{|e| \varepsilon_{in}}{W(\hbar\omega)^2 \varepsilon_{out}} \int_{+0}^{\infty} V' \Psi_0 \Psi_{1\mp} dz \right) \mathcal{E}_{in}^{(n)}, \quad (1)$$

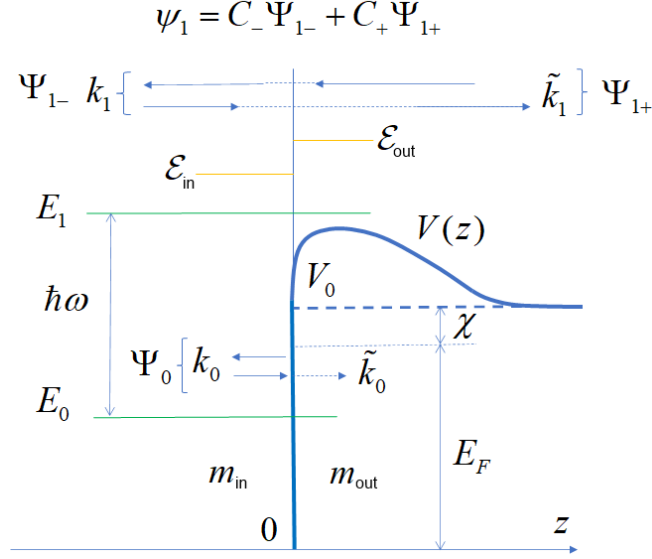


Figure 1. Electron from metal moves toward and collides with potential barrier $V(z)$ on metal ($z < 0$) - semiconductor ($z > 0$) interface in $z = 0$. Electron absorbs a photon of energy $\hbar\omega$ from electromagnetic field. $V(z)$ has a step change from 0 to V_0 in $z = 0$, $V \rightarrow V_0$ at $z \rightarrow +\infty$, V_0 is the energy of bottom of conductive band of semiconductor. $V_0 = E_F + \chi$, E_F is Fermi-energy and χ is a work function. Medium dielectric function $\varepsilon(z)$ and electron effective mass $m(z)$ have step changes in $z = 0$ between values ε_{out} , m_{out} for $z > 0$ and ε_{in} , m_{in} for $z < 0$. E_0 (E_1) are energies of the electron in initial (final) states of absorption. Ψ_0 is initial wave-function of the electron with the wave-number k_V (\tilde{k}_0) at $z < 0$ ($z > 0$). Ψ_{1+} and Ψ_{1-} are wave-functions of electron in basic final states with wave-numbers k_1 at $z < 0$ and \tilde{k}_1 at $z \rightarrow +\infty$, $\Psi_{0,1\pm}$ are calculated without electromagnetic field. ψ_1 is the wave-function of final state of an electron after absorption of a photon.

where $\mathcal{E}_{in}^{(n)}$ is the amplitude of the component of electric field inside the metal normal to the interface and

$$c_{\pm}^{(0)} = \frac{|e|}{(\hbar\omega)^2} \frac{m}{m_{in}W} \left\{ \left[(r_{\varepsilon}r_m - 1) \left(E_0 + \frac{\hbar\omega}{2} \right) - r_{\varepsilon}r_m V_0 \right] \Psi_0 \Psi_{1\mp} + (r_{\varepsilon} - 1) m_{in} \frac{\hbar^2 \Psi_0' \Psi_{1\mp}'}{2m^2} \right\} \Big|_{z=0}^{(2)},$$

where $r_{\varepsilon} = \varepsilon_{in}/\varepsilon_{out}$, $r_m = m_{in}/m_{out}$, W/m does not depend on z and $\Psi_0' \Psi_{1\mp}'/m^2$ is continuous function of z also in $z = 0$. Expression (2) follows from Eq.(2) of [13] as shown in Appendix. The second term in Eq.(1) describes the interaction of an electron with potential barrier $V(z)$ at $z > 0$. We suppose that discontinuities in $V(z)$, ε and m are in $z = 0$; m and ε at $z > 0$ and $z < 0$ are constant. Notations used in Eq.(2) are shown and explained in the caption of Fig.1.

Wave-functions $\Psi_0, \Psi_{1\pm}$ are solutions of the "unperturbed" Schrodinger equation

$$\left[-\frac{\hbar^2}{2} \frac{d}{dz} \left(\frac{1}{m} \frac{d}{dz} \right) + V(z) \right] \Psi(z) = E\Psi(z). \quad (3)$$

without the interaction with electromagnetic field. The first term on the left in Eq.(3) is kinetic energy operator of electron with varied effective mass $m(z)$. In Eq. (2) Ψ_0 is the wave function of the electron in initial state, $\Psi_0(z < 0) = e^{ik_V z}$ with the wave number $k_V = \sqrt{2m_{in}E_0}/\hbar$ and the energy $E = E_0$. The final state of the electron after absorption of a photon is

$$\psi_1 = C_+(z)\Psi_{1+}(z) + C_-(z)\Psi_{1-}(z),$$

where Ψ_{1+} (Ψ_{1-}) describe the electron with the energy $E_1 = E_0 + \hbar\omega$, which is moving to the right (to the left) far from the interface. C_+ is the probability amplitude of SPE, so Ψ_{1+} is normalized such that $\Psi_{1+}(z \rightarrow \infty) \rightarrow e^{i\tilde{k}_1 z}$ is the electron of photo-emission current with wave number $\tilde{k}_1 = \sqrt{2m_{out}(E_1 - V_0)}/\hbar$ moving to the right in the semiconductor conduction band. C_- is the probability amplitude of SPA, Ψ_{1-} is normalized such that $\Psi_{1-}(z < 0) = e^{-ik_1 z}$ corresponds to the electron reflected from the barrier and moving to the left in the metal with the wave number $k_1 = \sqrt{2m_{in}E_1}/\hbar$, such electron contributes to SPA. Wronskian

$$W(\Psi_{1-}, \Psi_{1+}) = \Psi_{1-} \frac{d\Psi_{1+}}{dz} - \Psi_{1+} \frac{d\Psi_{1-}}{dz},$$

and W/m does not depend on z [13]. In Eq.(2) prime means the derivative over z .

B. Results for 3D case

In 3D case an electron moves at arbitrary angle to the metal-semiconductor interface and the electromagnetic field is not necessary perpendicular to the interface. We factorize 3D wave functions

$$\Psi_i(z) e^{i\vec{k}_{\parallel} \vec{\rho}}, \quad (4)$$

where indexes $i = \{0, 1+, 1-\}$ have the same meaning as in 1D case, $e^{i\vec{k}_{\parallel} \vec{\rho}}$ describes the motion of an electron parallel to the interface, $\vec{k}_{\parallel} = \{\vec{e}_x k_x, \vec{e}_y k_y\}$, $\vec{\rho} = \{\vec{e}_x x, \vec{e}_y y\}$ and \vec{e}_x, \vec{e}_y are unit vectors of Cartesian coordinate system with axes x, y parallel to the interface. Approximation (4) has been used in [1, 2] supposing that potential barrier is averaged over

x and y and "flat" in these directions. In "flat" approximation $V(z)$, medium dielectric function ε and electron effective mass m do not depend on x and y and $\exp(i\vec{k}_{\parallel}\vec{\rho})$ and \vec{k}_{\parallel} in Eq. (4) remain the same as in the initial state of an electron.

Multipliers $\Psi_{0,1\pm}(z)$ in Eq. (4) are solutions of Eq. (3), which describes the motion of an electron perpendicular to the interface. In Eq. (3) initial energy E of an electron must be replaced by $E_z = (\hbar k_z)^2/2m_{in}$, which is the part of kinetic energy related with the motion of electron in metal perpendicular to the interface, k_z is z-component of the electron wave vector. Only the component of electromagnetic field perpendicular to the interface interacts with the electron, so the energy of photon, absorbed by electron, comes to the motion of electron perpendicular to the interface. A part of kinetic energy of electron in the final state, related with the motion perpendicular to the interface, is $E_{1z} = E_z + \hbar\omega$.

The second term in Eq. (1) is the same both for 1D and for 3D cases. In Eq.(2) for $c_{\pm}^{(0)}$ E_0 must be replaced by $E_z = (\hbar k_z)^2/2m_{in}$ and V_0 replaced by

$$V_z = V_0 + \frac{\hbar^2 k_{\parallel}^2}{2} \left(\frac{1}{m_{out}} - \frac{1}{m_{in}} \right). \quad (5)$$

The replacement (5) is a consequence of the momentum conservation law, which preserves k_{\parallel} , while an electron passes through "flat" interface with the discontinuity of electron effective mass. Such discontinuity requires the change in the electron velocity and, therefore, in the electron kinetic energy, which effectively increases the potential barrier causing the replacement $V_0 \rightarrow V_z$.

Only electrons with $E_z + \hbar\omega > V_z$ pass the barrier on the interface and contribute to SPE. z -component of velocity of such electrons far from the barrier is $\hbar\tilde{k}_{1z}/m_{out}$ where

$$\tilde{k}_{1z} = \sqrt{[k_z^2 + k_{\omega}^2 - k_V^2 - k_{\parallel}^2(r_m - 1)]/r_m}, \quad k_{\omega} = \sqrt{2m_{in}\omega/\hbar}, \quad k_V = \sqrt{2m_{in}V_0/\hbar}. \quad (6)$$

Now we derive the expression for SPE and SPA currents (or rates) in electrons per second. We consider "cold" electrons with initial energies in small interval $E_0 \div E_0 + dE_0$. A part of such electrons participate in SPE and SPA and make photo-currents with differential surface densities

$$dJ_{SPE,SPA} = |\mathcal{E}_{in}^{(n)}|^2 dj_{SPE,SPA}, \quad (7)$$

where

$$dj_{SPE} = \frac{\hbar \operatorname{Re}(\tilde{k}_{1z})}{m_{out}} |c_+|^2 dn_s, \quad dj_{SPA} = \frac{\hbar k_{1z}}{m_{in}} |c_-|^2 dn_s, \quad (8)$$

are differential photo-current surface densities per unit of $|\mathcal{E}_{in}^{(n)}|^2$, which is the part of the field energy density related with the component of the field inside metal normal to the interface,

$$dn_s = f_F(k_0^2)[1 - f_F(k_0^2 + k_\omega^2)] \frac{2k_{\parallel} dk_{\parallel} dk_z}{(2\pi)^2} \quad (9)$$

is a number of "cold" electrons in the unit of volume in small interval of energies, which can absorb a photon, $f_F(k_0^2)[1 - f_F(k_0^2 + k_\omega^2)]$ is the probability that the initial state of an electron with the energy $E_0 = (\hbar k_0)^2/2m_{in}$ is occupied and the final state with the energy $E_1 = \hbar^2(k_0^2 + k_\omega^2)/2m_{in}$ is free; $k_0^2 = k_z^2 + k_{\parallel}^2$, $k_{1z} = \sqrt{k_z^2 + k_\omega^2}$. In Eq.(8) we take real part of \tilde{k}_{1z} because of SPE exists only for electrons with kinetic energy above the minimum of the energy of semiconductor conductive band, so when

$$k_z^2 + k_\omega^2 - k_V^2 - k_{\parallel}^2(r_m - 1) > 0, \quad (10)$$

and \tilde{k}_{1z} is real. In Eq. (9)

$$f_F(y) = \left[1 + \exp \frac{\hbar^2 y / 2m_{in} - E_F}{K_B T} \right]^{-1} \quad (11)$$

is Fermi-distribution function, K_B is Boltzmann constant and T is a temperature.

In order to obtain total photo-currents J_{SPE} of SPE and J_{SPA} of SPA we integrate differential photo-current densities $dJ_{SPE,SPA}$ over states of all electrons colliding with nanoparticle surface, i.e. over dk_{\parallel} , dk_z , and over the nanoparticle surface with the area S_p . In the flat approximation $dj_{SPE,SPA}$ are the same in any point of the surface, so

$$J_{SPE,SPA} = \int_{k_z, k_{\parallel}} dj_{SPE,SPA} \int_{S_p} |\mathcal{E}_{in}^{(n)}|^2 dS_p \quad (12)$$

Internal quantum efficiency of SPE or SPA is

$$\eta_{SPE,SPA} = J_{SPE,SPA} / R_{abs} \quad (13)$$

where

$$R_{abs} = \int_{V_p} r_{abs} dV \quad (14)$$

is the rate of absorption in the volume V_p of a nanoparticle,

$$r_{abs} = \frac{\varepsilon''_{in}}{2\pi\hbar} |\mathcal{E}_{in}|^2 \quad (15)$$

is the absorption rate in the unit of volume, ε''_{in} is imaginary part of the dielectric function of metal. Combining expressions (12) – (15) we find

$$\eta_{SPE,SPA} = \frac{2\pi\hbar}{\varepsilon''_{in}a} \int_{k_z, k_{\parallel}} dj_{SPE,SPA}, \quad (16)$$

where the length

$$a = \int_{V_p} |\mathcal{E}_{in}|^2 dV_p / \int_{S_p} |\mathcal{E}_{in}^{(n)}|^2 dS_p. \quad (17)$$

In general a depends on the field. For small spherical nanoparticles with uniform electric field inside, a is nanoparticle radius.

It is convenient to introduce dimensionless variables

$$x_z = (k_z/k_V)^2, \quad x_{\parallel} = (k_{\parallel}/k_V)^2, \quad x_{\omega} = (k_{\omega}/k_V)^2 = \hbar\omega/V_0, \quad x_F = E_F/V_0 \quad (18)$$

and write

$$\eta_{SPE} = \frac{\eta_s}{\sqrt{r_m}} \int \text{Re} \sqrt{x_z + x_{\omega} - 1 - x_{\parallel}(r_m - 1)} |\tilde{c}_+|^2 d\tilde{n}_s \quad \eta_{SPA} = \eta_s \int \sqrt{x_z + x_{\omega}} |\tilde{c}_-|^2 d\tilde{n}_s, \quad (19)$$

An electron passes the barrier at SPE if η_{SPE} is real, so that when

$$x_z + x_{\omega} - 1 - x_{\parallel}(r_m - 1) > 0, \quad (20)$$

this is why we take the real part in the first of Eqs. (19). There

$$\eta_s = \frac{\lambda/a}{(2\pi)^2 \varepsilon''_{in}} \frac{e^2}{\hbar c} \left(\frac{V_0}{\hbar\omega} \right)^3, \quad d\tilde{n}_s = \tilde{f}_F(x) [1 - \tilde{f}_F(x + x_{\omega})] \frac{dx_{\parallel} dx_z}{\sqrt{x_z}}, \quad (21)$$

where λ is wavelength of applied field in vacuum, $e^2/\hbar c \approx 1/137$ is fine structure constant.

For gold nanoparticle in p-doped silica, considered in [13], $\eta_s = 1$ for $a = 15$ nm near localized plasmon resonance $\lambda = 0.857$ μm . Fermi distribution function

$$\tilde{f}_F(x) = \left[1 + \exp\left(\frac{x - x_F}{x_T}\right) \right]^{-1}, \quad x_F = E_F/V_0, \quad x_T = K_B T/V_0 \quad (22)$$

and

$$\tilde{c}_\pm = \tilde{c}_\pm^{(0)} - \frac{\varepsilon_{in} k_V}{V_0 W \varepsilon_{out}} \int_{+0}^{\infty} V' \Psi_0 \Psi_{1\mp} dz, \quad (23)$$

$$\tilde{c}_\pm^{(0)} = \frac{m k_V}{m_{in} W} \left\{ \left[(r_\varepsilon r_m - 1) \left(x_z + \frac{x_\omega}{2} \right) - r_\varepsilon r_m [1 + x_\parallel (r_m - 1)] \right] \Psi_0 \Psi_{1\mp} + (r_\varepsilon - 1) m_{in} \frac{\hbar^2 \Psi'_0 \Psi'_{1\mp}}{2m^2 V_0} \right\} \Big|_{z=0}. \quad (24)$$

While we write Eq. (24) we replace in Eq. (2) E_0 by $E_z = (\hbar k_z)^2/2m_{in}$ and V_0 by V_z given by Eq. (5).

SPE increases, when a nanoparticle became smaller. We display the dependence on the nanoparticle size explicitly and represent

$$\eta_s = a_s/a, \quad a_s(x_\omega) = a_{s0} \frac{\varepsilon''_{rb}}{\varepsilon''(x_\omega)} \left(\frac{1 - x_F}{x_\omega} \right)^4, \quad a_{s0} = \frac{\lambda_{rb}}{(2\pi)^2 \varepsilon''_{rb}} \frac{e^2}{\hbar c} \frac{1}{(1 - x_F)^3}, \quad (25)$$

where $\lambda_{rb} = 2\pi c/\omega_{rb}$ corresponds to the red border of photoemission, ε''_{rb} is $\varepsilon''(\omega_{rb})$, $e^2/(\hbar c) \approx 1/137$ is fine structure constant. Coefficient $\eta_s > 1$ when a size of nanoparticle $a < a_s$. At first approximation, we suppose that surface photoemission became important, when $\eta_s > 1$ so that $a < a_s$. Later we will find more precise estimation for the maximum a . a_s depends on the frequency of applied field, while a_{s0} does not so a_{s0} gives an estimation for the maximum size of a nanoparticle (in given environment), when SPE became comparable with VPE. $a_{s0} = 42$ nm for gold spherical nanoparticle in a semiconductor (like GaAs) with parameters as in [15] $V_0 = 6.31$ eV, $E_F = 5.51$ eV, $\varepsilon_{out} = 13$, gold dielectric function

$$\varepsilon_{Au}(\lambda) = 12 - \left(\frac{\lambda}{\lambda_p} \right)^2 \frac{1}{1 + i\lambda/\lambda_c} \quad (26)$$

used in [13], with $\lambda_p = 0.136$ μm , $\lambda_c = 55$ μm . Fig. 2 shows $a_s(\hbar\omega)$ for such parameters of nanoparticle.

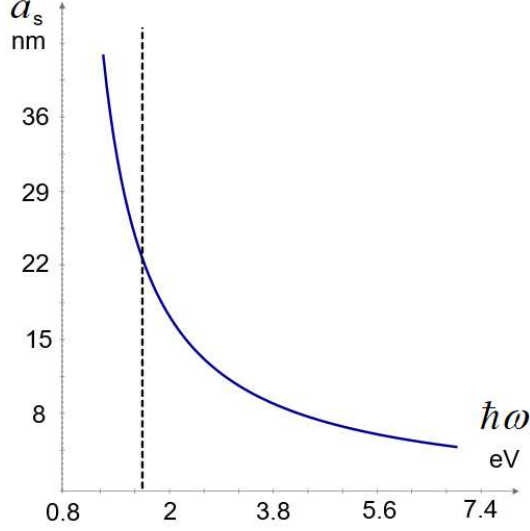


Figure 2. SPE became compatible with VPE, when the radius of nanoparticle $a < a_s(\omega)$ shown in the figure. Vertical dashed line marks localized plasmon resonance.

C. SPE and SPA with rectangular-step potential barrier

Wave functions $\Psi_{0,\pm}$ for rectangular potential barrier $V = 0, z < 0, V = V_0, z > 0$ are well-known and given, for example, in [13]. With such wave functions we find $(\Psi_0\Psi_{1\pm})_{z=0}$, $[\Psi'_0\Psi'_{1\pm}/m^2]_{z=0}$, see Appendix, and obtain

$$C_{\pm}^{(0)} = \frac{|e|}{im_{in}\omega^2} u(k_z) K_{\pm}^{dis}(k_z, k_{\parallel}), \quad (27)$$

with

$$u = \frac{k_z}{\left\{ k_z + i\sqrt{r_m[k_V^2 + k_{\parallel}^2(r_m - 1) - k_z^2]} \right\} \left\{ \sqrt{k_z^2 + k_{\omega}^2} + \sqrt{r_m[k_z^2 + k_{\omega}^2 - k_V^2 - k_{\parallel}^2(r_m - 1)]} \right\}} \quad (28)$$

where

$$K_{\pm}^{dis} = (r_{\varepsilon}r_m - 1) \left(k_z^2 + \frac{k_{\omega}^2}{2} \right) - r_{\varepsilon}r_m [k_V^2 + k_{\parallel}^2(r_m - 1)] \pm i(r_{\varepsilon} - 1) K_{\pm} \sqrt{r_m[k_V^2 + k_{\parallel}^2(r_m - 1) - k_z^2]}, \quad (29)$$

with

$$K_+ = \sqrt{k_z^2 + k_{\omega}^2}, \quad K_- = r_m \sqrt{k_z^2 + k_{\omega}^2 - k_V^2 - k_{\parallel}^2(r_m - 1)}.$$

We take dimensionless variables $x_z = (k_z/k_V)^2$, $x_{\parallel} = (k_{\parallel}/k_V)^2$, $x_{\omega} = (k_{\omega}/k_V)^2$ and express

$$\eta_{SPE} = \frac{a_s \sqrt{r_m}}{a} \int_0^{\infty} dx_{\parallel} \int_0^{\infty} \frac{dx_z}{\sqrt{x_z}} \operatorname{Re} \left[\sqrt{x_z + x_{\omega} - 1 - x_{\parallel}(r_m - 1)} \right] |\tilde{u} \tilde{K}_+^{dis}|^2 \tilde{f}_F(x) [1 - \tilde{f}_F(x + x_{\omega})],$$

$$\eta_{SPA} = \frac{a_s}{a} \int_0^{\infty} dx_{\parallel} \int_0^{\infty} \frac{dx_z}{\sqrt{x_z}} \sqrt{x_z + x_{\omega}} |\tilde{u} \tilde{K}_-^{dis}|^2 \tilde{f}_F(x) [1 - \tilde{f}_F(x + x_{\omega})],$$

where $x = x_z + x_{\parallel}$ is normalized energy of an electron,

$$\tilde{u} = \frac{\sqrt{x_z}}{\left\{ \sqrt{x_z} + i\sqrt{r_m} [1 + x_{\parallel}(r_m - 1) - x_z] \right\} \left\{ \sqrt{x_z + x_{\omega}} + \sqrt{r_m} [x_z + x_{\omega} - 1 - x_{\parallel}(r_m - 1)] \right\}}. \quad (30)$$

$$\tilde{K}_{\pm}^{dis} = (r_{\varepsilon} r_m - 1) \left(x_z + \frac{x_{\omega}}{2} \right) - r_{\varepsilon} r_m [1 + x_{\parallel}(r_m - 1)] \pm i(r_{\varepsilon} - 1) \tilde{K}_{\pm} \sqrt{r_m [1 + x_{\parallel}(r_m - 1) - x_z]}, \quad (31)$$

with

$$\tilde{K}_+ = \sqrt{x_z + x_{\omega}}, \quad \tilde{K}_- = r_m \sqrt{x_z + x_{\omega} - 1 - x_{\parallel}(r_m - 1)}.$$

We set $r_m = 1$ and obtain $\tilde{K}_+^{dis} = -K_{\Delta\varepsilon}$, where $K_{\Delta\varepsilon}$ given by Eq. (17) of [15] and $|\tilde{u}(x_z)|^2$ the same as $G(x_z)$ given by Eq. (16) of [15].

D. Surface photoemission near the red border

We neglect by the temperature dependence of electrons and set $T = 0$ then

$$\eta_{SPE} = \frac{a_s \sqrt{r_m}}{a} \left(\int_{1-x_{\omega}}^{x_{z0}} \int_0^{x_{\parallel 0}(x_z)} + \int_{x_{z0}}^{x_F} \int_0^{x_F - x_z} \right) dx_z dx_{\parallel} \frac{|\tilde{u} \tilde{K}_+^{dis}|^2}{\sqrt{x_z}} \sqrt{x_z + x_{\omega} - 1 - x_{\parallel}(r_m - 1)}, \quad (32)$$

where

$$x_{z0} = x_F + (1 - x_{\omega} - x_F)/r_m, \quad x_{\parallel 0}(x_z) = (x_z + x_{\omega} - 1)/(r_m - 1),$$

the area of integration in Eq. (32) is shown in Fig. 4. Near the red border of photoemission $x_z \approx x_F$, $x_{\parallel} \approx 0$, and $x_z + x_{\omega} \approx 1$, see Fig. 4. Near the red border we approximate

$$\tilde{u} \approx \frac{1}{1 + i\sqrt{r_m}(1 - x_F)/x_F}, \quad \tilde{K}_+^{dis} \approx (r_{\varepsilon} r_m - 1)(x_F + 1)/2 - r_{\varepsilon} r_m + i(r_{\varepsilon} - 1) \sqrt{r_m(1 - x_F)}, \quad (33)$$

and $\sqrt{x_z} \approx \sqrt{x_F}$. We use approximations (33), take $|\tilde{u}\tilde{K}_+^{dis}|^2/\sqrt{x_z}$ out of the integral in (32), calculate

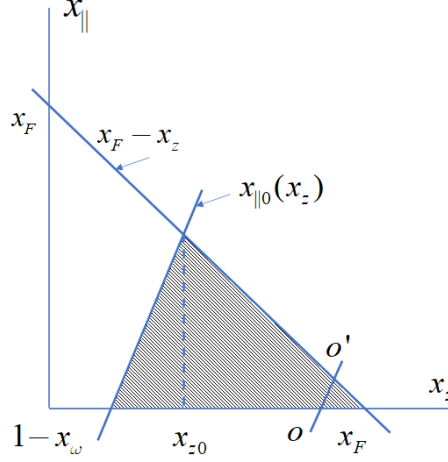


Figure 3. Area of integration in Eq. (32) is shadowed, $\max [x_{||}(x_z)] = (x_z + x_\omega - 1)/(r_m - 1)$. The line oo' restrict integration area at small excess of photon energy $x_\omega - x_W \ll x_F$ above the red border of photoemission, then $x_z \approx x_F$ and $x_{||} \approx 0$.

$$\int_0^y dx_{||} \sqrt{x_z + x_\omega - 1 - x_{||}(r_m - 1)} = \frac{2}{3(r_m - 1)} \left\{ (x_z + x_\omega - 1)^{3/2} - [x_z + x_\omega - 1 - (r_m - 1)y]^{3/2} \right\}, \quad (34)$$

take the rest of integrals in Eq. (32) and obtain

$$\eta_{SPE} = \frac{a_{s0}}{a} \frac{4\sqrt{x_F}}{15} F_{\varepsilon m} \frac{\delta x_\omega^{5/2}}{\sqrt{r_m}}, \quad F_{\varepsilon m} = \frac{[1 + x_F + r_\varepsilon r_m(1 - x_F)]^2/4 + (r_\varepsilon - 1)^2 r_m(1 - x_F)}{x_F + r_m(1 - x_F)}. \quad (35)$$

Here $\delta x_\omega = x_\omega - x_W \ll 1$ is a part of photon energy above the barrier, $F_{\varepsilon m} = 1$ when $r_m = r_\varepsilon = 1$ and near the red border we take $a_s = a_{s0}$. Fig. 4 shows $\eta_{SPE}(\omega)$ given by Eq. (32) and its approximation near the red border (35) for gold nanoparticle of radius $a = 8.4$ nm in semiconductor like GaAs with $\varepsilon_{out} = 13$. One can see that SPE spectrum $\eta_{SPE} \sim \delta x_\omega^{5/2}$, which is good approximation in small region of $\hbar\omega$ near the red border.

III. VOLUME PHOTO-EMISSION

We consider the volume photo-emission (VPE) for small spherical nanoparticles following [15]. We suppose, that only electrons of metal absorb photons. Then the rate of absorption

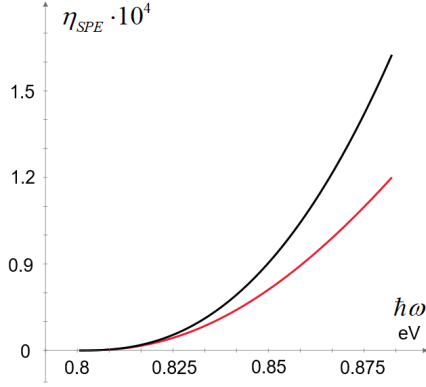


Figure 4. η_{SPE} for rectangular potential barrier. Exact curve Eq. (32) (red) and its approximation (35) near the red border (black).

r_{abs} given by Eq. (15) is also the rate of generation of hot electrons in the unit of volume. The rate of photoemission of hot electrons from the unit of volume is

$$r_{VPE} = r_{abs} W_t W_p, \quad (36)$$

where W_t is the probability that hot electron, avoiding inelastic collisions, reaches the nanoparticle surface, and W_p is the probability that hot electrons passes through the barrier on the surface and leaves the nanoparticle. The rate of photoemission from the nanoparticle is

$$R_{VPE} = \int_{V_p} r_{abs} \langle W_t W_p \rangle dV, \quad (37)$$

where

$$\langle W_t W_p \rangle = \frac{1}{n_h} \int W_t W_p f_h g d^3 k$$

is the average over parameters of hot electrons with distribution function f_h , density of states $g = 2/(2\pi)^3$ in the unit of volume, $d^3 k = k^2 dk \sin \theta d\theta d\varphi$ and where $n_h = \int f_h g d^3 k$ is the number of hot electron states in the unit of volume. Internal quantum efficiency of VPE is

$$\eta_{VPE} = R_{VPE}/R_{abs} \quad (38)$$

where R_{abs} is the rate (14) of absorption of photons in nanoarticle. We consider small spherical nanoparticles, where the energy density of electric field $|E_{in}|^2$ is constant. Combyning

Eqs (37), (38) and (14) we express

$$\eta_{VPE} = \frac{1}{n_h V_p} \int W_t W_p f_h g d^3 k dV. \quad (39)$$

Parameters of hot electrons in the volume of small nanoparticle are same, therefore $W_p f_h g$ in Eq. (39) does not depend on spatial coordinates so we simplify Eq. (39) by separating the integrations

$$\eta_{VPE} = \frac{1}{n_h} \int \overline{W}_t W_p f_h g d^3 k, \quad \overline{W}_t = \frac{1}{V_p} \int W_t dV. \quad (40)$$

Following [4, 12] we approximate the distribution of hot electrons by homogeneous distribution over energies from E_F to $E_F + \hbar\omega$ so $f_h = 1$ for $k_F^2 < k^2 < k_F^2 + k_\omega^2$ and $f_h = 0$ otherwise. Nothing depends on angular coordinates in space and on azimuthal angle in k -

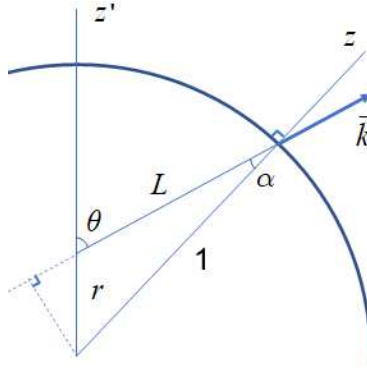


Figure 5. Spherical coordinate system in k -space for volume photoemission with z -axes z' and polar angle θ . Axis z is normal to the nanoparticle surface in the point, when electron leaves nanoparticle. The distance r is from the center of nanoparticle to the point of generation of hot electron. All distances are normalized to nanoparticle radius taken 1 in the Figure.

space in spherical nanoparticle, the integration over these variables in Eq. (39) gives 4π and 2π , respectively. We calculate

$$n_h = 4\pi \int_{k_F}^{k_h} \frac{2}{(2\pi)^3} k^2 dk = \frac{k_h^3 - k_F^3}{3\pi^2}, \quad V_p = 4\pi/3, \quad k_h^2 = k_F^2 + k_\omega^2$$

and write integrals in Eq. (39) in coordinates shown in Fig. 4

$$\eta_{VPE} = \frac{9}{2(k_h^3 - k_F^3)} \int_0^1 r^2 dr \int_{k_V}^{k_h} k^2 dk \int_0^\pi \sin \theta d\theta W_t(r, \theta) \text{Re} [W_p(k, \theta)]. \quad (41)$$

Here and below we use dimensionless spatial coordinate r normalised to nanoparticle radius. Taking $\text{Re}[W_p(k, \theta)]$ in Eq. (41) we consider there only hot electrons passing the barrier, such electrons fly in the cone with $0 < \alpha < \alpha_m$ (see α in Fig.5) [8]. For such electrons $W_p(k, \theta)$ is real, otherwise $W_p(k, \theta)$ is purely imaginary. We take dimensionless energies

$$x = E/V_0, \quad x_F = E_F/V_0, \quad x_h = (E_F + \hbar\omega)/V_0 \quad (42)$$

and re-write Eq. (41) in terms of them. In general $W_p(k, \theta) \neq W_p(x, \theta)$ but, for simplicity, we keep the same notations for $W_p(k, \theta)$ and $W_p(x, \theta)$ and in other similar cases.

$$\eta_{VPE} = \frac{9}{4(x_h^{3/2} - x_F^{3/2})} \int_0^1 r^2 dr \int_1^{x_h} \sqrt{x} dx \int_0^\pi \sin \theta d\theta W_t(r, \theta) \text{Re}[W_p(x, \theta)], \quad (43)$$

Following [15] we suppose that hot electron moves ballistically without elastic collisions, and it can not be emitted if it loses the energy in single inelastic collision. Then the probability that hot electron reaches the nanoparticle boundary is

$$W_t(r, \theta) = \exp[-L(r, \theta)/l_e], \quad (44)$$

where $L(r, \theta) = \sqrt{1 - r^2 \sin^2 \theta} - r \cos \theta$ is the length of the way of hot electron to the interface shown in Fig. 5, r is the distance from the nanoparticle center to the point of generation of hot electron, and l_e is the mean free path of an electron in metal, r and l_e are normalized to radius of spherical nanoparticle.

We simplify Eq. (43) and represent it according with Eq. (40). First, we separate the integration region over $d\theta$ in Eq.(43) in two parts: from 0 to $\pi/2$ and from $\pi/2$ to π . Probability W_p that hot electron passes the barrier depends on normalised kinetic energy x of the electron and on the part $x \sin^2 \alpha$ of this energy, correspondent to the motion parallel to the interface, therefore $W_p = W_p(x, \sin^2 \alpha)$. We note that $\sin^2 \alpha = r^2 \sin^2 \theta$ (see Fig. 5) and introduce in Eq. (43) new variable $y = r^2 \sin^2 \theta$ instead of θ so that $W_p = W_p(x, y)$. We come from θ to y in Eqs. (43), (44), taking into account that $\sin \theta d\theta = dy/(2r\sqrt{r^2 - y})$, introduce $z = r^2$ and after that separate integrations in η_{VPE} as in (40)

$$\eta_{VPE} = \frac{9}{4(x_h^{3/2} - x_F^{3/2})} \int_1^{x_h} \sqrt{x} dx \int_0^{y_m(x)} \overline{W}_t(y) W_p(x, y) dy \quad (45)$$

where

$$\overline{W}_t(y) = \frac{1}{4} \int_y^1 \frac{dz}{\sqrt{z-y}} W_t(z, y) \quad (46)$$

with

$$W_t = \exp\left(-\sqrt{1-y}/l_e\right) \left[\exp\left(-\sqrt{z-y}/l_e\right) + \exp\left(\sqrt{z-y}/l_e\right)\right], \quad (47)$$

for W_t initially given by Eq. (44). The integral (46) can be taken and we obtain

$$\overline{W}_t(y) = \frac{l_e}{2} \left[1 - \exp\left(-\frac{2\sqrt{1-y}}{l_e}\right)\right]. \quad (48)$$

Now we determine $y_m(x)$ in Eq. (45). The energy of hot electron in metal is $(\hbar k)^2/2m_{in}$. When the electron passes through the barrier, the component $k \sin \alpha$ of its wave vector is preserved, while the component k_z normal to the interface is not preserved. Z-component \tilde{k}_z of the wave vector of emitted electron outside the metal, far from the barrier, is found from the energy conservation law

$$\hbar^2(\tilde{k}_z^2 + k^2 \sin^2 \alpha)/2m_{out} + V_0 = (\hbar k)^2/2m_{in}. \quad (49)$$

Taking $\sin \alpha = r \sin \theta$, see Fig. 5, we obtain from Eq. (49)

$$\tilde{k}_z = \sqrt{[k^2(1 - r_m r^2 \sin^2 \theta) - k_V^2]/r_m}. \quad (50)$$

\tilde{k}_z must be real, so only electrons with $k > k_V$ and inside a cone with $\sin \theta < \sin \theta_m$ pass through the barrier. From Eq. (50) we obtain

$$r^2 \sin^2 \theta < r^2 \sin^2 \theta_m \equiv y_m(x) = (1 - 1/x)/r_m, \quad x = k^2/k_V^2 \quad (51)$$

We suppose, for simplicity, $r_m > 1$ which is typical case for semiconductor-metal interface, then $0 < y_m(x) < 1$. With the result (48) we obtain

$$\eta_{VPE} = \frac{9l_e}{8(x_h^{3/2} - x_F^{3/2})} \int_1^{x_h} \sqrt{x} dx \int_0^{(1-1/x)/r_m} \left[1 - \exp\left(-\frac{2\sqrt{1-y}}{l_e}\right)\right] W_p(x, y) dy. \quad (52)$$

Since we do not know l_e precisely, we can ignore y-dependence in $\exp(-\sqrt{1-y}/l_e)$ in

Eq. (52) and write in good approximation

$$\eta_{VPE} = \frac{9l_e[1 - \exp(-2/l_e)]}{8(x_h^{3/2} - x_F^{3/2})} \int_1^{x_h} \sqrt{x} dx \int_0^{(1-1/x)/r_m} W_p(x, y) dy. \quad (53)$$

This result can be used with arbitrary $W_p(x, y)$ supposing that W_t is given by Eq. (44).

A. VPE with rectangular-step potential barrier

We calculate the wave function of hot electron in the coordinate system with axes z , normal to the nanoparticle surface shown in Fig. 5, as we did for SPE and SPA. Similar with the wave-functions (4) for SPE, the wave function of hot electron in VPE is factorized as $\Psi_z(z)e^{i\vec{k}_{\parallel}\vec{\rho}}$. In Fig.5 we see that

$$k_{\parallel} = k \sin \alpha, \quad k_z = k \cos \alpha \quad (54)$$

are components of the wave-vector of hot electron, parallel and perpendicular to the surface, the wave number of hot electron is k . Z-dependent part of the wave function is

$$\Psi_z(z) = (e^{ik_z z} + Ae^{-ik_z z})_{z < 0} + (Be^{i\tilde{k}_z z})_{z > 0}, \quad (55)$$

where A and B are c-number constants. z -component \tilde{k}_z of the wave-vector for $z > 0$ is given by Eq. (50). Inserting the wave function (55) into the boundary conditions at $z = 0$ $\Psi_h(-0) = \Psi_h(+0)$ and $m_{in}^{-1}(d\Psi_h/dz)_{z=-0} = m_{out}^{-1}(d\Psi_h/dz)_{z=+0}$ we obtain $B = 2/(1 + r_m \tilde{k}_z/k_z)$. With the wave-function (55) the fluxes of electrons in z -direction toward (away from) the barrier are $j_z^{(in)} = \hbar k_z/m_{in}$ ($j_z^{(out)} = (\hbar \tilde{k}_z/m_{out})|B|^2$) so the probability that hot electron passes through the barrier is

$$W_p(k, k_z) \equiv j_z^{(out)}/j_z^{(in)} = \frac{4r_m k_z \operatorname{Re} \tilde{k}_z}{(k_z + r_m \tilde{k}_z)^2}, \quad (56)$$

if conditions (51) are true and $W_p = 0$ otherwise. Using dimensionless variables (42) and $y = r^2 \sin^2 \theta$ we write

$$W_p(x, y) = \frac{4\sqrt{r_m x(1-y)[x(1-r_m y) - 1]}}{\left\{ \sqrt{x(1-y)} + \sqrt{r_m[x(1-r_m y) - 1]} \right\}^2}. \quad (57)$$

Volume photoemission efficiency η_{VPE} is given by (53).

B. VPE near the red border

Here we consider volume photoemission near the red border, when absorption of photons gives small excess of the hot electron energy above the barrier $\delta x_\omega = (\hbar\omega + E_F)/V_0 - 1 \ll 1$. Then $x = 1 + \delta x$, $\delta x \ll 1$, $y \ll 1$ and we approximate W_p in Eq. (57) as

$$W_p \approx 4\sqrt{r_m} \sqrt{\delta x_\omega - r_m y} \quad (58)$$

Inserting Eq. (58) into Eq. (53) we take integrals we obtain

$$\eta_{VPE} \approx \frac{6 l_e [1 - \exp(-2/l_e)]}{5} \cdot \frac{\delta x_\omega^{5/2}}{1 - x_F^{3/2} \sqrt{r_m}}. \quad (59)$$

We see that near the red border of photoemission $\eta_{VPE} \sim 1/\sqrt{r_m}$. Such dependence of η_{VPE} on the electron effective mass is weaker than the result (26) of [8] where $\eta_{VPE} \sim 1/r_m$ near the red border. This difference is because of in Eq. (26) of [8] $R_{eff}(0)$ (the analog of our $W_p \sim \sqrt{r_m}$) does not depend on r_m . The change in the effective mass (for $r_m > 1$) effectively increases the potential barrier on the interface, because the momentum conservation law requires acceleration of the motion of electrons parallel to the interface, while they pass the barrier. However the same acceleration increases the flux of electrons in the normal direction out of the surface and therefore increases photoemission, this is why our $W_p \sim \sqrt{r_m}$. Overall influence of the decrease of effective mass on the photoemission is still negative, because the pass of the barrier requires the addition of the electron kinetic energy proportional to the square of electron velocity.

Near the red border the spectra of SPE and VPE are the same $\sim \delta x_\omega^{5/2}$. However approximations (35) and (58) are valid only in a small interval of frequencies near the

red border. Analytical approximation for η_{VPE} valid in larger region of frequencies of applied field is obtained by taking

$$W_p \approx \frac{4\sqrt{r_m}\sqrt{\delta x_\omega - r_m y}}{(1 + \sqrt{r_m}\sqrt{\delta x_\omega - r_m y})^2}. \quad (60)$$

and $\sqrt{x} \approx 1$ in Eq. (53). Then integrals in Eq. (53) can be calculated and we find

$$\eta_{VPE} = \frac{18l_e(1 - e^{-2/l_e})}{r_m^2(1 - x_F^{3/2})} \left[\delta x_\omega(1 + \sqrt{r_m\delta x_\omega}/3) - 2\sqrt{\delta x_\omega/r_m} + \ln(\sqrt{r_m\delta x_\omega} + 1)(2/r_m - \delta x_\omega) \right]. \quad (61)$$

Comparing approximations (58) and (61) we see that dependencies $\eta_{VPE}(\delta x_\omega, r_m)$ not very close to the red border strongly depend on the expression for the probability W_p that hot electron passes the barrier. The same is true for SPE, where we do not yet find an analytic approximation similar to (61).

Fig. 6 shows η_{VPE} given by Eq. (52), its approximation (58) near the red border and more precise approximation (61) for $l_e = 0.5$ (in units of nanoparticle radius).

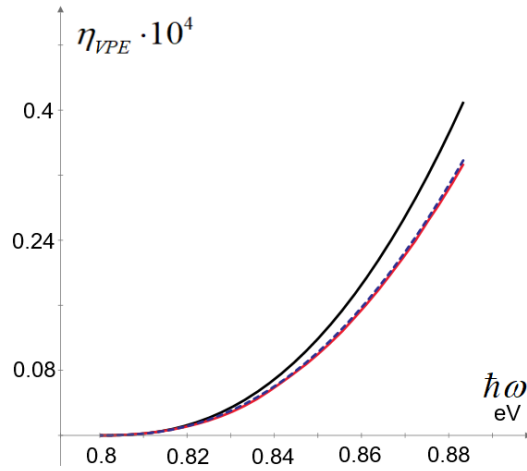


Figure 6. Internal quantum efficiency of volume photoemission (53) with exact rectangular step barrier (57) (red curve), its approximation near the red border (59) (black curve) and with more precise approximation (61) (blue dashed curve).

IV. COMPARISON OF EFFICIENCIES OF SPE AND VPE

Comparing Fig. 4 with Fig. 6 we see that near the red border $\eta_{SPE} > \eta_{VPE}$, so SPE is more efficient than VPE for gold nanoparticle of diameter less than $2a = 15$ nm correspondent to these figures. Equating Eqs. (35) and (59) we find the maximum nanoparticle radius $a_{rb}(r_m, r_\varepsilon)$, when efficiencies $\eta_{VPE} = \eta_{SPE}$ on the red border

$$a_{rb}(r_m, r_\varepsilon) = a_{s0} \frac{2\sqrt{x_F}}{9} F(r_m, r_\varepsilon) \frac{1 - x_F^{3/2}}{l_e [1 - \exp(-2/l_e)]}, \quad (62)$$

where $F(r_m, r_\varepsilon)$ is given by Eq. (35). Therefore SPE will be more efficient than VPE on the red border for spherical gold nanoparticles of radius $a < a_{rb}$ in given semiconductor environment. Note in Fig 7 that larger jump in the environment dielectric function $|r_\varepsilon| =$

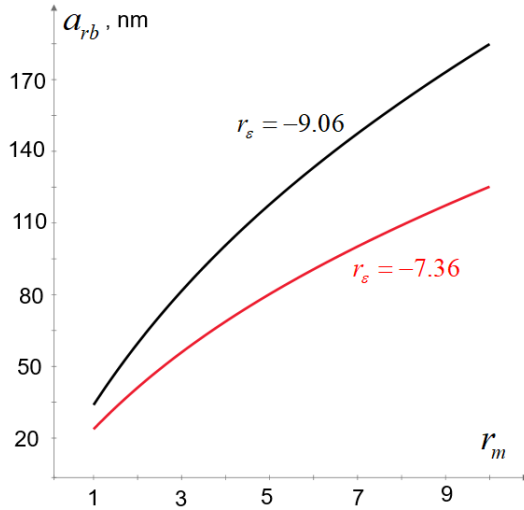


Figure 7. Nanoparticle radius a_{rb} , when $\eta_{SPE} = \eta_{VPE}$ so SPE and VPE have the same efficiencies on the red border of photoemission. SPE is more efficient than VPE on the red border for nanoparticles of radius $a < a_{rb}$. Black curve is for gold nanoparticle in the semiconductor with $\varepsilon_{out} = 13$, red curve is for $\varepsilon_{out} = 16$. As larger is $|r_\varepsilon|$ as larger is the nanoparticle with $\eta_{SPE} = \eta_{VPE}$ on the red border.

$|\varepsilon_{in}/\varepsilon_{out}|$ corresponds larger nanoparticle radius a_{rb} when $\eta_{SPE} = \eta_{VPE}$.

Fig 8 shows spectra of $\eta_{SPE}(\omega)$ (32) and $\eta_{VPE}(\omega)$ (53) for $\varepsilon_{out} = 13$ and $\varepsilon_{out} = 16$ for $r_m = 2$ and nanoparticle of diameter $2a = 15$ nm. We a region where photon energy is not too high and where SPE is more efficient than VPE $\eta_{SPE} > \eta_{VPE}$. Such region includes plasmon resonance frequency. For high frequency $\eta_{SPE} < \eta_{VPE}$.

Fig. 9 shows η_{SPE} and η_{VPE} as functions of the jump in the electron effective mass

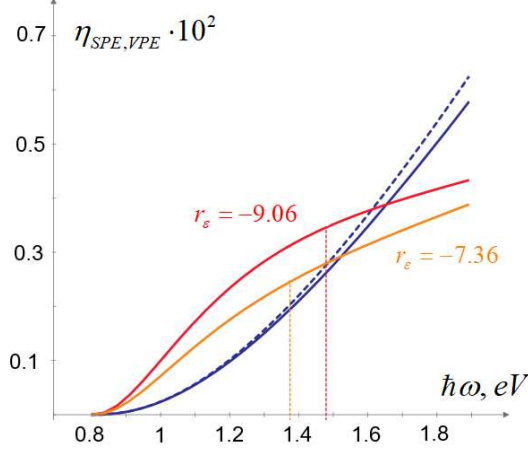


Figure 8. Spectra of internal quantum efficiencies of SPE (blue curves) and SPE (red and orange curves) given by Eqs. (53) and (32), respectively. Blue dashed curve is approximation (61) for η_{VPE} . Vertical dotted lines mark plasmon resonance frequencies. The red curve is for gold nanoparticle in *GaAs*-like semiconductor, the red curve – in silica. The change in electron effective mass on the interface is $r_m = 2$, diameter of spherical nanoparticle $2a = 15$ nm, the electron mean free pass $l_e = 0.5a$. $\eta_{SPE} > \eta_{VPE}$ if photon frequency is not too high, also for localised plasmon resonance.

r_m for gold spherical nanoparticle in *GaAs*-like semiconductor with $\varepsilon_{out} = 13$ or in silica environment with $\varepsilon_{out} = 16$ at plasmon resonance frequency (specific for the environment). Both SPE and VPE efficiencies decrease with r_m , but η_{SPE} decreases slowly than η_{VPE} . Because of that SPE is more efficient: $\eta_{SPE} > \eta_{VPE}$ apart of small region of r_m near $r_m = 1$.

In Figs. 8, 9 and 7 we see that SPE efficiency is larger for larger break $|r_\varepsilon|$ in the electromagnetic field (EMF). This is because of the absorption of photons by electrons, interacting with EMF discontinuity, is added to the absorption at collisions of electrons with potential barrier on the interface [15] at SPE. Absorption at EMF discontinuity is reverse process to well-known transition radiation, when a charged particle passes through inhomogeneous media, for example through a boundary between two different media [5].

Slow decrease of η_{SPE} with r_m , respectively to fast decrease of η_{VPE} , is because of the electron wave vector component $k_{||}$, preserved on the interface, remains small and the same as for cold electron in case of SPE. In other words, hot electrons must be accelerated, due to the momentum conservation law, passing the interface at VPE, while "cold" electrons require such acceleration at SPE. So less energy is taken for the acceleration in the case of SPE than in VPE. In more details, the electron at SPE interacts only with normal component of EMF, and the energy of absorbed photon comes only to the motion of electron normal

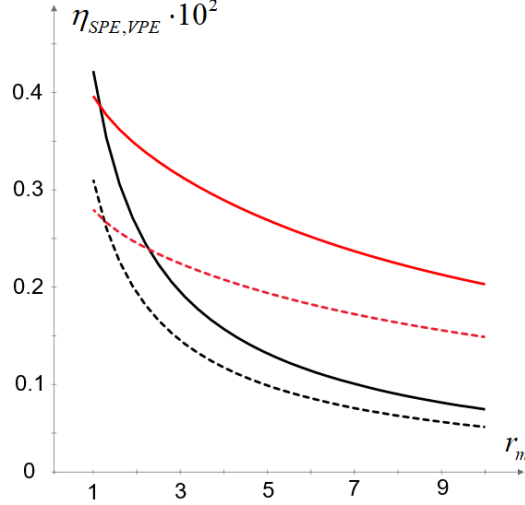


Figure 9. Quantum efficiencies of SPE (red curves) and VPE (black curves) as functions of the electron effective mass change r_m on the metal-semiconductor interface. Solid curves are for gold nanoparticle in *GaAs*-like semiconductor, dashed curves correspond to silica semiconductor environment. The difference in η_{VPE} (black curves) in different environment is related with different plasmon resonance frequency. $\eta_{SPE} > \eta_{VPE}$ everywhere apart of small region near $r_m = 1$.

to the interface. Such motion is affected by the potential barrier, so it does not obey by the momentum conservation law and therefore it is not accelerated due to $m_{in} > m_{out}$. By contrast, in VPE the energy of absorbed photon is, in average, equally distributed among all directions of motion: 1/3 of that energy comes to the direction normal to the interface and 2/3 goes to directions parallel to the interface. In case of VPE the motion parallel to the interface requires acceleration if $r_m > 1$. So in order to preserve the momentum parallel to the interface at mass discontinuity, cold electron must have more energy in case of VPE than in case of SPE.

We express $x_z = x_0 \cos^2 \alpha$, $x_{\parallel} = x_0 \sin^2 \alpha$ and $x = x_0 + x_{\omega}$, where $x_0 = E_0/V_0$ is normalized energy of cold electron before absorption of photon (in the volume or on the surface), $x_{\omega} = \hbar\omega/V_0$ and α is the angle of incidence of an electron on the nanoparticle surface as shown in Fig. 5. Then we rewrite conditions (20) for SPE and (51) (with $r^2 \sin^2 \theta = \sin^2 \alpha$) for VPE as, respectively

$$\sin^2 \alpha < \sin^2 \alpha_{SPE} = \delta x_{\omega}/(r_m x_0), \quad \sin^2 \alpha < \sin^2 \alpha_{VPE} = \delta x_{\omega}/[r_m(x_0 + x_{\omega})] \quad (63)$$

where $\delta x_{\omega} = x_0 + x_{\omega} - 1$ is excess of the hot electron energy above the barrier and $\alpha_{SPE,VPE}$ are maximum angles of cones of flying electrons for VPE and SPE. We see that

$\sin^2 \alpha_{SPE} / \sin^2 \alpha_{VPE} = 1 + x_\omega / x_0 > 1$, so that the cone of electrons available for SPE is larger than for VPE.

V. SUMMARY

Decrease of electron effective mass in the semiconductor environment of metal nanoparticle reduces the surface and the volume photoemission (SPE and VPE) as a consequence of the momentum conservation law, which requires additional energy from an electron and effectively increases the potential barrier. We find that such reduction for VPE is larger than for SPE. The reason is that the energy of absorbed photon at SPE is contributed to the electron motion normal to the interface, the conservation of momentum is not required in this direction. The motion of electron along the interface, subjected by the momentum conservation law, is not accelerated by absorption of photon. In contrast, the motion of electrons in all directions is equally accelerated at photon absorption in the volume. The conservation of momentum parallel to the interface requires larger electron velocity outside the metal and, correspondingly, larger energy of electrons in metal in VPE than in SPE. So less electrons are available for photoemission for VPE than for SPE. We provide general formulas for internal quantum efficiencies of SPE and VPE with an account for discontinuities in electron effective mass, dielectric function and potential barrier in the metal-environment interface of metal nanoparticle. We derive analytical formulas for the quantum efficiencies on the red border of photoemission. Using these formulas we compared SPE and VPE from gold spherical nanoparticle in semiconductors with rectangular potential barrier on the interface and find conditions when SPE is more efficient than VPE.

Results can be used for modelling, investigation and optimisation of conditions of generation of "hot" electrons at the absorption of electromagnetic field by metal nanoparticles, for calculations of broadening of localized plasmon resonances by collisions of electrons with nanoparticle surface and for heating of nanoparticles by the radiation.

ACKNOWLEDGMENTS

A.V.U. acknowledges the Russian Science Foundation (Grant No. 20-19-00559) and I.E.P. thanks Russian Foundation for Basic Research (Grant No. 21-58-15011) for support.

APPENDIX

Derivation of formulas (1) and (2)

Following [13] we write

$$C_{\pm} = \frac{|e|m}{W(\hbar\omega)^2} \int_{-\infty}^{\infty} \frac{dz}{m} (c_V + c_{\mathcal{E}} + c_m) \quad (64)$$

where

$$\begin{aligned} c_V &= -\mathcal{E}V'\Psi_0\Psi_{1\mp} \\ c_{\mathcal{E}} &= \mathcal{E}' \left[\frac{\hbar^2}{2m} \Psi_0'\Psi_{1\mp}' + \left(E_0 - V + \frac{\hbar\omega}{2} \right) \Psi_0\Psi_{1\mp} \right] \\ c_m &= -\frac{\mathcal{E}m'}{m} \left(E_0 - V + \frac{\hbar\omega}{2} \right) \Psi_0\Psi_{1\mp}. \end{aligned} \quad (65)$$

We insert (65) into (64) and find

$$C_{\pm} = \frac{|e|m}{W(\hbar\omega)^2} \int_{-\infty}^{\infty} dz \left\{ \left[-\left(\frac{\mathcal{E}V}{m} \right)' + \left(E_0 + \frac{\hbar\omega}{2} \right) \left(\frac{\mathcal{E}}{m} \right)' \right] \Psi_0\Psi_{1\mp} + \mathcal{E}' \frac{\hbar^2 \Psi_0'\Psi_{1\mp}'}{2m^2} \right\}. \quad (66)$$

If $f(z)$ is discontinues function in $z = 0$, $f(+0) = f_+$, $f(-0) = f_-$ then $f'(z)_{z=0} = (f_{+0} - f_{-0})\delta(0)$. We consider a product of discontinues functions as single discontinues function. Therefore $(\mathcal{E}V/m)'_{z=0} = (\mathcal{E}_{out}V_0/m_{out})\delta(0)$, taking into account that $V(z < 0) = 0$; $(\mathcal{E}/m)'_{z=0} = (\mathcal{E}_{out}/m_{out} - \mathcal{E}_{in}/m_{in})\delta(0)$. From boundary conditions $\varepsilon_{in}\mathcal{E}_{in} = \varepsilon_{out}\mathcal{E}_{out} = \mathcal{E}_n$, therefore $\mathcal{E}_{in}/\mathcal{E}_{out} = \varepsilon_{out}/\varepsilon_{in}$. After integration in (66) we obtain result (1) with $C_{\pm}^{(0)}$ given by (2).

Wave functions for rectangular step potential barrier

For rectangular-step potential (5) multipliers $\Psi_{z_0,1\pm}$ in wave functions (4) are obtained from wave functions $\Psi_{0,1\pm}$ of 1D problem [13] by replacement $V_0 \rightarrow V_z$

$$\begin{aligned} \Psi_0(z) &= [\exp(ik_z z) + A_0 \exp(-ik_z z)]_{z < 0} + B_0 \exp(-\tilde{k}_z z)_{z > 0}, \\ \Psi_{1+}(z) &= [A_{1+} \exp(ik_{1z} z) + B_{1+} \exp(-ik_{1z} z)]_{z < 0} + \exp(i\tilde{k}_{1z} z)_{z > 0} \\ \Psi_{1-}(z) &= [A_{1-} \exp(i\tilde{k}_{1z} z) + B_{1-} \exp(-i\tilde{k}_{1z} z)]_{z > 0} + \exp(-ik_{1z} z)_{z < 0} \end{aligned}$$

$\tilde{k}_z = \sqrt{[k_V^2 + k_{\parallel}^2(r_m - 1) - k_z^2]/r_m}$ is real, $k_{1z} = \sqrt{k_z^2 + k_{\omega}^2}$, $\tilde{k}_{1z} = \sqrt{[k_z^2 + k_{\omega}^2 - k_V^2 - k_{\parallel}^2(r_m - 1)]/r_m}$,
 $r_m = m_{in}/m_{out}$

$$A_0 = (1 - i\theta_0)/(1 + i\theta_0), \quad B_0 = 2/(1 + i\theta_0),$$

$$A_{1-} = (1 + \theta_1)/2, \quad B_{1-} = (1 - \theta_1)/2,$$

$$A_{1+} = (\theta_1 - 1)/2\theta_1, \quad B_{1+} = (1 + \theta_1)/2\theta_1$$

and

$$\theta_0 = \sqrt{r_m(V_z/E_z - 1)}, \quad \theta_1 = \sqrt{r_m[1 - V_z/(E_z + \hbar\omega)]}.$$

so that

$$(\Psi_0\Psi_{1\pm})_{z=0} = B_0 = \frac{2\sqrt{E_z}}{\sqrt{E_z + i\sqrt{r_m(V_z - E_z)}}} = \frac{2k_z}{k_z + i\sqrt{r_m[k_V^2 + k_{\parallel}^2(r_m - 1) - k_z^2]}}.$$

$$\left. \frac{\Psi'_0\Psi'_{1-}}{m^2} \right|_{z=0} = \frac{i\tilde{k}_z k_{1z}}{m_{out}m_{in}} B_0 = i \frac{\sqrt{[k_V^2 + k_{\parallel}^2(r_m - 1) - k_z^2](k_{\omega}^2 + k_z^2)}}{m_{in}\sqrt{m_{out}m_{in}}} B_0,$$

$$\left. \frac{\Psi'_0\Psi'_{1+}}{m^2} \right|_{z=0} = -\frac{i\tilde{k}_z \tilde{k}_{1z}}{m_{out}^2} B_0 = -i \frac{\sqrt{[k_V^2 + k_{\parallel}^2(r_m - 1) - k_z^2][k_z^2 + k_{\omega}^2 - k_V^2 - k_{\parallel}^2(r_m - 1)]}}{m_{out}\sqrt{m_{out}m_{in}}} B_0,$$

and

$$\frac{W(z)}{m(z)} = \frac{ik_1}{m_{in}}(1 + \theta_1) = \frac{1}{m_{in}} \left\{ \sqrt{k_z^2 + k_{\omega}^2} + \sqrt{r_m [k_z^2 + k_{\omega}^2 - k_V^2 - k_{\parallel}^2(r_m - 1)]} \right\}$$

-
- [1] A. M. Brodskii and Yu. Ya. Gurevitch. Theory of external photoeffect from the surface of a metal. Soviet Physics JETP, 27:114–121, 1968.
- [2] A Brodsky and Yu Gurevich. Teoriya Elektronnoi Emissii iz Metallov (Theory of Electron Emission from Metals). Moscow, Nauka, 1973.
- [3] Mark Brongersma, Naomi Halas, and Peter Nordlander. Plasmon-induced hot carrier science and technology. Nature nanotechnology, 10:25–34, 01 2015.
- [4] R. H. Fowler. The analysis of photoelectric sensitivity curves for clean metals at various temperatures. Phys. Rev., 38:45–56, Jul 1931.

- [5] V L Ginsburg and I M Frank. Radiation of a uniformly moving electron due to its transition from one medium into another. JETP (USSR), 16:15–28, 1946.
- [6] Matthias Graf, Dirk Jalas, Jerg Weissmeijler, Alexander Yu Petrov, and Manfred Eich. Surface-to-volume ratio drives photoelectron injection from nanoscale gold into electrolyte. ACS Catalysis, 9(4):3366–3374, 2019.
- [7] Renat Sh. Ikhsanov, Igor E. Protsenko, Igor V. Smetanin, and Alexander V. Uskov. Landau broadening of plasmonic resonances in the mie theory. Opt. Lett., 45(9):2644–2647, May 2020.
- [8] Jacob B. Khurgin. Fundamental limits of hot carrier injection from metal in nanoplasmonics. Nanophotonics, 9(2):453 – 471, 01 Feb. 2020.
- [9] Minho Kim, Jung-Hoon Lee, and Jwa-Min Nam. Plasmonic photothermal nanoparticles for biomedical applications. Advanced Science, 6(17):1900471, 2019.
- [10] Charles Kittel. Introduction to Solid State Physics. Wiley, 8 edition, 2004.
- [11] Christian Kuppe, Kristina R. Rusimova, Lukas Ohnoutek, Dimitar Slavov, and Ventsislav K. Valev. Hot in plasmonics: Temperature-related concepts and applications of metal nanostructures. Advanced Optical Materials, 8(1):1901166, 2020.
- [12] A. Novitsky, A. V. Uskov, C. Gritti, I. E. Protsenko, B. E. Kardynal, and A. V. Lavrinenko. Photon absorption and photocurrent in solar cells below semiconductor bandgap due to electron photoemission from plasmonic nanoantennas. Progress in Photovoltaics: Research and Applications, 22(4):422–426, 2014.
- [13] Igor E Protsenko and Aleksandr V Uskov. Photoemission from metal nanoparticles. Physics-Uspekhi, 55(5):508–518, may 2012.
- [14] I. Tamm and S. Schubin. Zur theorie des photoeffektes an metallen. Z Phys, 68:97–113, 1931.
- [15] Alexander V. Uskov, Igor E. Protsenko, Renat S. Ikhsanov, Viktoriia E. Babicheva, Sergei V. Zhukovsky, Andrei V. Lavrinenko, Eoin P. O’Reilly, and Hongxing Xu. Internal photoemission from plasmonic nanoparticles: comparison between surface and volume photoelectric effects. Nanoscale, 6:4716–4727, 2014.
- [16] Alexander V. Uskov, Igor E. Protsenko, N. Asger Mortensen, and Eoin P. O’Reilly. Broadening of plasmonic resonance due to electron collisions with nanoparticle boundary: a quantum mechanical consideration. Plasmonics, 9(1):185–192, Feb 2014.
- [17] Sergei V. Zhukovsky, Viktoriia E. Babicheva, Alexander V. Uskov, Igor E. Protsenko, and Andrei V. Lavrinenko. Enhanced electron photoemission by collective lattice resonances in

plasmonic nanoparticle-array photodetectors and solar cells. Plasmonics, 9(2):283–289, Apr 2014.